

Positron cooling via inelastic collisions in CF₄ and N₂ gases

A. R. Swann* and D. G. Green†

School of Mathematics and Physics, Queen's University Belfast, University Road, Belfast BT7 1NN, United Kingdom

(Dated: January 8, 2022)

Positron cooling via inelastic collisions in CF₄ and N₂ gases is simulated, including positron-positron interactions. Owing to the molecular symmetries, cooling is assumed to be chiefly due to energy loss via vibrational (rotational) excitations for CF₄ (N₂). For CF₄, it is found that the inclusion of the dipole-inactive ν_1 mode, in addition to the dipole-active modes ν_3 and ν_4 , can provide room-temperature thermalization and an accurate cooling timescale. Combination cooling enabled by the ν_1 mode, and positron-positron interactions both contribute to the Maxwellianization of the positron momentum distribution. For both gases the evolution of the positron temperature is found to be in excellent agreement with experiment.

The development of the positron buffer-gas trap in the 1980s [1] has enabled the routine trapping, accumulation, and delivery of positrons in beams [2, 3]; the study of low-energy antimatter-matter interactions with atoms and molecules, including scattering, binding, and annihilation [4, 5]; and the formation and exploitation of positronium [6, 7] and antihydrogen [8]. Positrons from a ²²Na source (with energies 0–500 keV) are slowed to eV energies by passing through an ~8 K solid-neon moderator, then magnetically guided into the three-stage buffer-gas trap. The first two stages contain N₂ gas in which the positrons cool, typically through electronic excitation [9]. In the third stage, a mixture of N₂ and CF₄ (or SF₆) is used to complete the thermalization of the positrons to room temperature, typically via rotational and vibrational excitation of the molecules [10]. They can be cooled further in a cryogenic beam-tailoring trap which produces an ultra-high resolution (~7 meV FWHM) energy-tunable beam [11].

Optimization of current traps, and development of next-generation traps, accumulators, beams and positron-based technologies require theoretical insight. The theory of low-energy positron cooling in atomic and molecular gases, however, lags well behind experiment (see, e.g., Refs. [12, 13] for early reviews). Most existing theoretical work has been for noble gases, for which the dominant positron-energy-loss mechanism is momentum transfer in elastic collisions. Solutions of the Fokker-Planck equation using model scattering cross sections [14–19] yielded limited agreement with experiment. Recently, however, a Monte Carlo approach employed by one of us that used accurate many-body-theory scattering cross sections gave a complete description of positron cooling in noble gases, finding excellent agreement with experiment for cooling rates, time-dependent annihilation rates [20], and γ spectra [21]. Cooling at higher energies in noble gases via electronic excitation, ionization, and positronium formation has also been investigated [22]. For molecular gases, less progress has been made, with even cooling in N₂ and CF₄ not well understood, though some simulations exist [23, 24].

Natisin *et al.* [25] performed measurements of positron cooling following microwave heating to ~1500 K in CF₄, N₂, and CO gases, finding that their results were consistent with a positron momentum distribution (PMD) that remained Maxwellian throughout the cooling process. For CF₄, their theoretical model (a simple differential equation for the mean

energy loss, assuming a Maxwellian PMD throughout) included only the dominant ν_3 mode: with this single vibrational channel, one should, however, expect the PMD to deviate significantly from Maxwellian as positrons below the vibrational excitation threshold cannot cool further, leading to a “pileup” of positrons just below the threshold. The mechanism(s) causing “Maxwellianization” is not yet understood.

Here, we calculate the evolution of the PMD and temperature during cooling in CF₄ and N₂ gases via inelastic collisions. For CF₄, we show that even when both dipole-active vibrational modes (ν_3 and ν_4) are included [26], pileups indeed occur, resulting in a non-Maxwellian PMD, and moreover, that the positrons do not even thermalize to room temperature. We explore two mechanisms that could effect Maxwellianization:

(1) Excitation of the dipole-inactive ν_1 mode. We find that this has a significant effect on the cooling, providing a pathway for positrons below the lowest excitation threshold to continue to cool, mitigating the pileup and leading to thermalization on the timescale observed in the experiment. It does not appear to be sufficient, however, to fully Maxwellianize the PMD.

(2) Positron-positron collisions. The relative importance of positron-positron and positron-gas collisions is governed by the ratio $R \equiv n_e/n_g$ of the positron number density n_e to the gas number density n_g . While positron-positron collisions are known to be capable of effecting rapid Maxwellianization at high positron densities [27], it is not clear *a priori* what magnitude of R is required for this to occur. We find that the density ratio in the CF₄ cooling experiment of Natisin *et al.* [25], $R \sim 10^{-7}$ – 10^{-6} [28], may be sufficient to noticeably enhance the Maxwellianization of the PMD, beyond the effect of including the ν_1 vibrational mode.

For N₂, we find that the PMD remains Maxwellian during cooling via rotational excitations of the molecules, even without positron-positron collisions.

Overall, we obtain excellent agreement with experiment for both CF₄ and N₂.

Simulation procedure.—The PMD $f(k, \tau)$, where k is the momentum and $\tau \equiv n_g t$ is the *time-density* (t being the time), normalized as $\int_0^\infty f(k, \tau) dk = 1$, is calculated as follows. We use the ANTICool program [29], modified to include vibrational and rotational inelastic positron-gas collisions, and positron-positron collisions. We employ a grid in τ with constant step size $\Delta\tau$. The initial momentum of

each positron is sampled from a Maxwell-Boltzmann distribution (MB) at ~ 1500 K, corresponding to the experiment [25]. In each time-density step, and for each positron, the probability of a collision with either a molecule or another positron is $P = W \Delta\tau$, where W is the total collision rate: $W = n_g [\int u \sigma_{eg}(u) f_g(\mathbf{v}') d\mathbf{v}' + R \int u \sigma_{ee}(u) f_e(\mathbf{v}') d\mathbf{v}']$, where $u \equiv |\mathbf{v} - \mathbf{v}'|$ is the relative speed of the incident positron and target gas molecule or positron, σ_{eg} and σ_{ee} are the positron-gas and positron-positron scattering cross sections, respectively, $f_g(\mathbf{v}')$ and $f_e(\mathbf{v}')$ are the velocity distributions of the gas molecules and positrons, respectively, and $\Delta\tau$ is chosen such that $W \Delta\tau \ll 1$ [30]. We approximate $\int u \sigma_{eg}(u) f_g(\mathbf{v}') d\mathbf{v}'$ by $v_{eg} \sigma_{eg}(v_{eg})$, where v_{eg} is the relative speed of the positron and a single gas molecule whose velocity is sampled from a MB at room temperature, $T_R = 300$ K. To calculate $\int u \sigma_{ee}(u) f_e(\mathbf{v}') d\mathbf{v}'$, we use the method of Weng and Kushner [31, 32]. A random number $r_1 \in [0, 1]$ is drawn, and if $r_1 < P$, then a collision is deemed to occur. If so, another random number $r_2 \in [0, 1]$ determines the target type: if $r_2 < n_g v_{eg} \sigma_{eg}(v_{eg}) / W$, the target is a molecule; otherwise, it is another positron. Finally, a random number $r_3 \in [0, 1]$ determines the specific scattering channel, i.e., the initial and final states of the molecule for an inelastic positron-gas collision, or the velocity of the target positron for a positron-positron collision [32]. In a positron-gas collision, the energy lost by the positron is $\varepsilon_f - \varepsilon_i$, where ε_i and ε_f are the energies of the initial and final states of the molecule, respectively; in a positron-positron collision, the energy change of the incident positron is determined by the relative speed of the two positrons and the scattering angle [31]. The temperature of the positrons at a given τ is calculated as $T = k_{\text{rms}}^2 / 3m_e k_B$, where k_{rms} is the root-mean-squared momentum of the positrons, m_e is the positron mass, and k_B is the Boltzmann constant.

Positron cooling in CF₄ gas.—Since CF₄ has T_d symmetry, its electric dipole and quadrupole moments are zero. Thus, positron cooling in CF₄ is expected to be predominantly via vibrational, rather than rotational, excitations of the molecules. CF₄ possesses four fundamental vibrational modes. Modes ν_1 and ν_2 , with energies $\varepsilon_1 = 113$ meV and $\varepsilon_2 = 53.9$ meV, are dipole inactive, while modes ν_3 and ν_4 , with energies $\varepsilon_3 = 159$ meV and $\varepsilon_4 = 78.4$ meV, are dipole active [33]. We investigate cooling of the positrons from 1700 K ($k_B T = 146$ meV) to 300 K ($k_B T = 26$ meV). For simplicity, we consider only fundamental transitions, and initially, we neglect the role of positron-positron collisions. We use the Born-dipole approximation for the transition cross sections $\sigma_{0 \rightleftharpoons 3,4}$ between the vibrational ground state ν_0 and dipole-active modes ν_3 and ν_4 [32, 34]. Semiempirical coupled-channel calculations [35] found $\sigma_{0 \rightarrow 3}$ to be similar in shape and magnitude to the corresponding Born-dipole calculation, but $\sigma_{0 \rightarrow 4}$ to be approximately four times larger than the corresponding Born-dipole calculation (see Fig. 6 in Ref. [35]). Therefore, we also perform calculations using the Born-dipole $\sigma_{0 \rightarrow 4}$ scaled by 4. For ν_1 , we are unaware of any theoretical or experimental investigation of positron-impact excitation, so we turn to a set of measurements of $\sigma_{0 \rightarrow 1,3,4}$ for *electron* im-

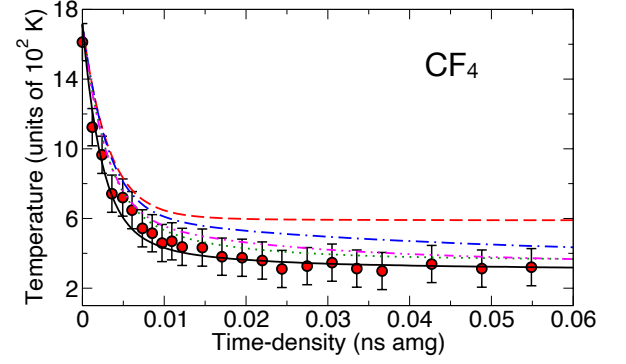


FIG. 1. Positron temperature during cooling in CF₄. Calculations in ν_3 (dashed red), $\nu_3 + \nu_4$ (dot-dashed blue), $\nu_3 + 4\nu_4$ (dotted green), $\nu_3 + \nu_4 + \nu_1$ (dot-dash-dotted magenta) and $\nu_3 + 4\nu_4 + 4\nu_1$ (solid black) approximations (see text), and experiment [25] (red circles).

pact [36] and assume the positron-impact cross sections to be similar in shape and magnitude to the electron-impact ones (as predicted for ν_3 and ν_4 [35]). The overall shape of each measured cross section is similar, differing in the threshold energy and magnitude. The peak in the measured $\sigma_{0 \rightarrow 1}$ is approximately 3.1 times higher than the peak in the measured $\sigma_{0 \rightarrow 4}$ (see Fig. 1 in Ref. [36]). Thus, we estimate $\sigma_{0 \rightleftharpoons 1}$ using the Born-dipole expressions for $\sigma_{0 \rightleftharpoons 4}$, scaled by 3.1. We carry out a second set of calculations where we scale $\sigma_{0 \rightleftharpoons 1}$ by a further factor of 4, to account for the fact that the Born-dipole calculation of $\sigma_{0 \rightarrow 4}$ is approximately four times smaller than the corresponding coupled-channel calculation [35] (see above). We are unaware of any existing calculations or measurements of $\sigma_{0 \rightleftharpoons 2}$, so we neglect these transitions entirely.

Figure 1 shows the calculated time-dependent positron temperature compared with experiment [25, 37]. The simulation used 200 000 positrons with $\Delta\tau = 2 \times 10^{-6}$ ns amg. The figure separately shows the results for when only the $0 \rightleftharpoons 3$ transitions are included; when the $0 \rightleftharpoons 3$ and $0 \rightleftharpoons 4$ transitions are included; and when the $0 \rightleftharpoons 3$, $0 \rightleftharpoons 4$, and $0 \rightleftharpoons 1$ transitions are included (denoted ν_3 ; $\nu_3 + \nu_4$; and $\nu_3 + \nu_4 + \nu_1$, respectively). Also shown are the results for when $\sigma_{0 \rightleftharpoons 4}$ and $\sigma_{0 \rightleftharpoons 1}$ are scaled by the factor of 4 to approximate the coupled-channel calculations (denoted $\nu_3 + 4\nu_4$ and $\nu_3 + 4\nu_4 + 4\nu_1$, respectively). The $\nu_3 + 4\nu_4 + 4\nu_1$ calculation gives excellent agreement with experiment. The other approximations predict slower cooling of the positrons. In fact, for ν_3 and $\nu_3 + \nu_4$, the positrons do not thermalize close to $T_R = 300$ K. The reason for this is most easily seen by considering $f(k, \tau)$ for a particular value of τ . Figure 2 shows $f(k, \tau)$ in the various approximations for $\tau = 0.06$ ns amg [see also the video [CF₄-video](#) in Supplemental Material [38]]. Also shown is the MB for $T = 1700$ K from which the positron momenta at $\tau = 0$ are sampled (dashed gray line), the peak of which almost coincides with the value of k corresponding to the $0 \rightarrow 3$ excitation threshold energy (rightmost dotted black line). In the ν_3 approximation, only positrons above this threshold can lose energy. Thus, at $\tau = 0.06$ ns amg, when equilibrium has

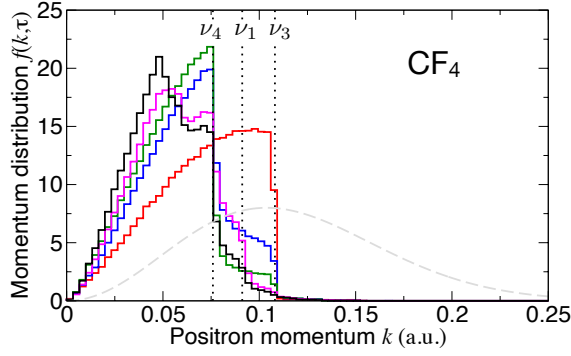


FIG. 2. Calculated PMD $f(k, \tau)$ at $\tau = 0.06$ ns amg for cooling in CF_4 in the ν_3 , $\nu_3 + \nu_4$, $\nu_3 + 4\nu_4$, $\nu_3 + \nu_4 + \nu_1$, and $\nu_3 + 4\nu_4 + 4\nu_1$ approximations (see text; colored as in Fig. 1). Also shown is the initial MB for $T = 1700$ K (dashed-gray line) and the vibrational excitation thresholds (dotted vertical lines).

been reached, we observe a pileup in $f(k, \tau)$ just below this threshold, with $f(k, \tau) \sim 0$ above the threshold. The positron temperature can thus decrease no further. In the $\nu_3 + \nu_4$ and $\nu_3 + 4\nu_4$ approximations, at $\tau = 0.06$ ns amg, we observe pileups below both thresholds. Both diminish on longer timescales than considered here: those just below the $0 \rightarrow 3$ threshold can cool via $0 \rightarrow 4$ excitation; those below the $0 \rightarrow 4$ threshold can cool, but only via *multiple* $4 \rightarrow 0$ deexcitations (since $2\varepsilon_4 < \varepsilon_3$) followed by a $0 \rightarrow 3$ excitation. The $\nu_3 + \nu_4 + \nu_1$ and $\nu_3 + 4\nu_4 + 4\nu_1$ approximations are notably different. The additional ν_1 mode enables positrons below the lowest ($0 \rightarrow 4$) excitation threshold to cool further via a *single* deexcitation and excitation of the molecule. For example, a positron with energy ε where $\varepsilon_1 - \varepsilon_4 < \varepsilon < \varepsilon_4$ can induce a $4 \rightarrow 0$ deexcitation followed by a $0 \rightarrow 1$ excitation, thus reducing its energy by $\varepsilon_1 - \varepsilon_4$; another pathway is via a $1 \rightarrow 0$ deexcitation followed by a $0 \rightarrow 3$ excitation. Since the deexcitation cross sections are orders of magnitude smaller than the excitation ones above the vibrational excitation thresholds [32], such cooling via a single deexcitation and excitation is much more probable than via multiple deexcitations followed by excitation. Indeed, the peak in $f(k, \tau)$ (at $k \approx 0.05$ a.u.) corresponds to the energy $\varepsilon_1 - \varepsilon_4$, below which positrons can cool further only via the improbable multiple deexcitations pathway. The doorway provided by the ν_1 mode thus appears to provide an accurate cooling timescale and room-temperature thermalization.

In all of the approximations, the PMD at equilibrium is markedly non-Maxwellian. This is because in inducing the vibrational transitions, the positrons lose or gain energy in large amounts relative to the overall energy spread of the PMD, e.g., the energy lost in a $0 \rightarrow 4$ excitation is $\sim 10\%$ of the initial overall spread of positron energies (assuming an initial momentum spread of $0 \leq k \leq 0.25$ a.u.; see Fig. 2). Figure 3 shows $f(k, \tau)$ for the best approximation, $\nu_3 + 4\nu_4 + 4\nu_1$, for several τ [see also the video [CF4-video](#) in Supplemental Material [38]]. The PMD for $\tau = 0.06$ ns amg (the final value of τ displayed), though close in shape and magnitude to the MB for $T_R = 300$ K, has a lingering pileup at the $0 \rightarrow 4$ threshold, pre-

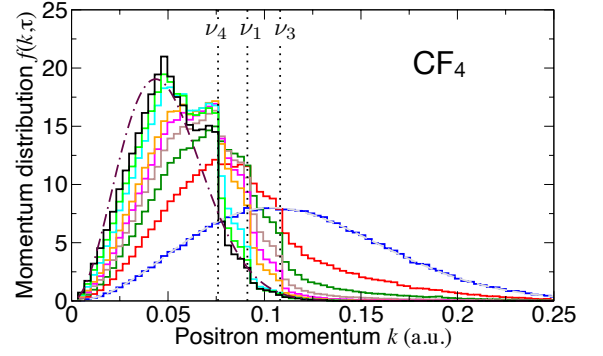


FIG. 3. Calculated PMD $f(k, \tau)$ for cooling in CF_4 , in the $\nu_3 + 4\nu_4 + 4\nu_1$ approximation at the following values of τ (in ns amg): 0 (blue), 0.002 (red), 0.004 (dark green), 0.006 (brown), 0.008 (magenta), 0.01 (orange), 0.02 (cyan), 0.03 (light green), 0.06 (black). Also shown is the initial MB for $T = 1700$ K (dashed gray line), the MB for $T_R = 300$ K (dot-dashed line) and the vibrational excitation thresholds (dotted vertical lines).

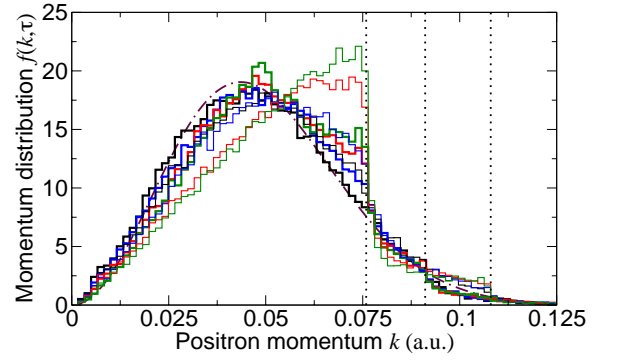


FIG. 4. Calculated PMD $f(k, \tau)$ at $\tau = 0.06$ ns amg for cooling in CF_4 with the inclusion of positron-positron interactions. Thin lines, $\nu_3 + 4\nu_4$ approximation; thick lines, $\nu_3 + 4\nu_4 + 4\nu_1$ approximation. Values of R : 1×10^{-6} (black), 5×10^{-7} (blue), 1×10^{-7} (red), 1×10^{-8} (green). Dot-dashed line, MB for $T_R = 300$ K.

cluding full Maxwellianization of the PMD. We now consider, therefore, the possible role of positron-positron collisions. Figure 4 shows $f(k, \tau)$ for $\tau = 0.06$ ns amg in the $\nu_3 + 4\nu_4$ and $\nu_3 + 4\nu_4 + 4\nu_1$ approximations, using 50 000 positrons, with the inclusion of positron-positron interactions, for $R = 10^{-8} - 10^{-6}$. For $R = 10^{-6}$, the positron-positron collisions clearly Maxwellianize the PMD in both approximations, eliminating the pileup at the $0 \rightarrow 4$ threshold almost completely. For $R = 10^{-7}$, however, the effect of positron-positron collisions is much smaller, and for $R = 10^{-8}$, the PMD in both approximations is essentially the same as it was without positron-positron collisions (cf. Fig. 2). Thus, in the experiment of Natisin *et al.* [25], since R is estimated to be $\sim 10^{-7} - 10^{-6}$ [28], positron-positron collisions may or may not play a significant role. Figure 5 shows the time dependence of the positron temperature in the $\nu_3 + 4\nu_4$ and $\nu_3 + 4\nu_4 + 4\nu_1$ approximations, with the inclusion of positron-positron interactions. For all values of R considered, even $R = 10^{-6}$, the $\nu_3 + 4\nu_4 + 4\nu_1$ approximation

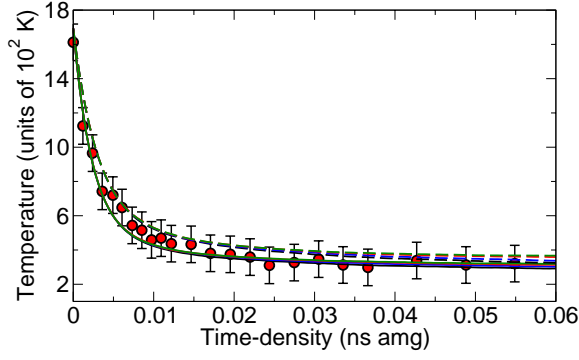


FIG. 5. Positron temperature during cooling in CF_4 with the inclusion of positron-positron interactions. Dashed lines, $\nu_3 + 4\nu_4$ approximation; solid lines, $\nu_3 + 4\nu_4 + 4\nu_1$ approximation (colored as in Fig. 4). Red circles, experiment [25].

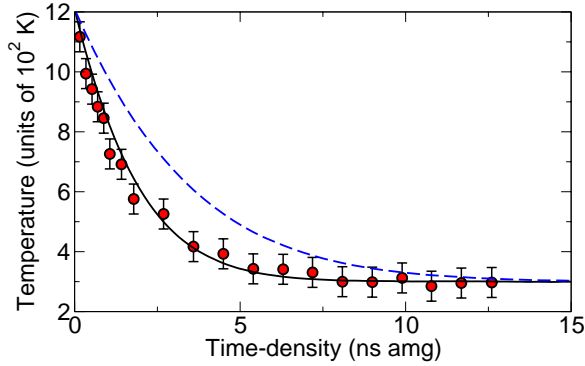


FIG. 6. Positron temperature during cooling in N_2 . Calculations with $J_{\text{max}} = 60$ using unscaled cross sections (dashed blue) and scaled cross sections (solid black); experiment [25] (red circles).

provides slightly better agreement with experiment than the $\nu_3 + 4\nu_4$ approximation.

Positron cooling in N_2 gas.—The homonuclear diatomic N_2 molecule has no permanent electric dipole moment, and its fundamental vibrational mode is dipole inactive. Therefore, we initially assume that positron cooling in N_2 proceeds via quadrupole rotational excitations. To a good approximation, the energy of a rotational level with angular momentum J is $\varepsilon_J = BJ(J+1)$, where B is the rotational constant. For N_2 , we take $B = 9.2 \times 10^{-6}$ a.u. [39]. We use the Born-quadrupole cross sections for the $J \rightleftharpoons J+2$ transitions [40], and we find that including up to $J = 60$ gives converged results [32]. We neglect the role of positron-positron collisions.

Figure 6 shows the calculated time-dependent positron temperature during cooling from an initial MB at 1200 K (corresponding to the experiment [25, 41]). We use 200 000 positrons and $\Delta\tau = 5 \times 10^{-4}$ ns amg. The calculation (dashed blue line) predicts slower cooling than the experiment (red circles). A similar phenomenon was observed in the theoretical model of Natisin *et al.* [25], suggesting that the Born-quadrupole approximation may underestimate the true rotational excitation cross sections. Natisin *et al.* found that scaling the Born-

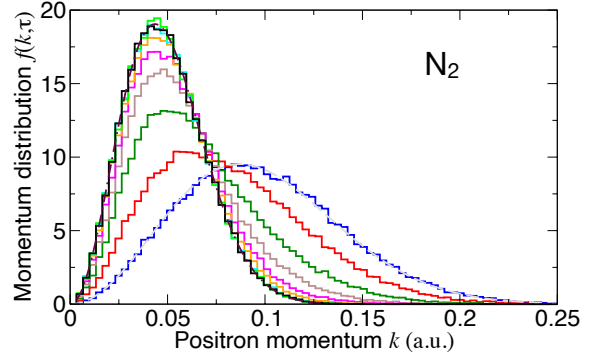


FIG. 7. Positron momentum distribution $f(k, \tau)$ for cooling in N_2 for τ as follows (in ns amg): 0 (blue), 0.9 (red), 2.1 (dark green), 3.3 (brown), 4.5 (magenta), 5.7 (orange), 8.1 (cyan), 10.5 (light green), 12.9 (black). Also shown in the initial MB for $T = 1200$ K (dashed gray line) and the MB for $T_R = 300$ K (dot-dashed maroon line).

quadrupole cross sections by an empirical factor of 1.8 gave much better agreement between the predictions of their model and their experimental data [25], and yielded a magnitude for $\sigma_{0 \rightarrow 2}$ in better agreement with calculation [42]. Thus, we likewise performed calculations with the Born-quadrupole cross sections scaled by 1.8 (solid black line in Fig. 6). Excellent agreement with the experiment is achieved; the thermalization time is consistent with the 14 ns amg measured in Ref. [43].

Figure 7 shows $f(k, \tau)$ for several values of τ [see also the video [N2-video](#) in Supplemental Material [44]]. In contrast to CF_4 , $f(k, \tau)$ for N_2 remains near-Maxwellian as τ proceeds. Moreover, R is ~ 30 times smaller in the experiment for N_2 than in the experiment for CF_4 , so positron-positron collisions will not play a significant role. Indeed, for the final value of τ shown, viz., $\tau = 12.9$ ns amg, $f(k, \tau)$ follows a MB for $T_R = 300$ K very closely. This is a result of the relatively small energy spacing between the various rotational levels in comparison to that between the vibrational levels in CF_4 .

Conclusions.—Positron cooling via inelastic collisions in CF_4 and N_2 gases—the buffer gases of choice in the ubiquitous Surko traps—has been studied via a Monte Carlo approach. Specifically, we simulated the experiment of Natisin *et al.* [25], where positrons cooled following microwave heating to ~ 1500 K. Cooling in CF_4 (N_2) was assumed to proceed via vibrational (rotational) excitations. For CF_4 , we found that including the two dipole-active modes ν_3 and ν_4 was insufficient. Because of the relatively large amounts of energy lost by the positron in inducing a discrete vibrational excitation, the PMD does not remain Maxwellian: pileups are observed near each of the vibrational excitation thresholds. We found that inclusion of the ν_1 mode can provide a doorway for further cooling, diminishing the pileups below the dipole-active thresholds and ultimately providing excellent agreement with experiment for the time dependence of the positron temperature. However, even with the inclusion of ν_1 , the PMD remains markedly non-Maxwellian. We found that positron-positron collisions can effect efficient Maxwellianization of the PMD

for $R = 10^{-6}$, but not for $R = 10^{-7}$ (or smaller), where R is the ratio of the positron and gas number densities. In the experiment, $R \sim 10^{-7}$ – 10^{-6} is estimated [28], so the importance of positron-positron collisions in the experiment is unclear. For N_2 , the energy spacing between the rotational levels is much smaller than that between the vibrational levels of CF_4 , so the distribution remains near-Maxwellian throughout the cooling. Improved calculations or measurements of the positron-impact transition cross sections between rovibrational levels would enable more definitive calculations of cooling. In principle, annihilation of positrons during the cooling is another process that can affect the overall PMD and positron temperature, but this is not expected to play a significant role for cooling in CF_4 and N_2 [45].

Acknowledgments.—We thank Cliff Surko and James Danielson for useful discussions regarding the experiment, and Gleb Gribakin for encouraging us to consider positron-positron interactions and providing useful comments on the draft manuscript. This work was supported by ERC StG 804383 “ANTI-ATOM”.

* a.swann@qub.ac.uk

† d.green@qub.ac.uk

- [1] C. M. Surko, M. Leventhal, and A. Passner, Positron Plasma in the Laboratory, *Phys. Rev. Lett.* **62**, 901 (1989).
- [2] S. J. Gilbert, C. Kurz, R. G. Greaves, and C. M. Surko, Creation of a monoenergetic pulsed positron beam, *Appl. Phys. Lett.* **70**, 1944 (1997).
- [3] J. R. Danielson, D. H. E. Dubin, R. G. Greaves, and C. M. Surko, Plasma and trap-based techniques for science with positrons, *Rev. Mod. Phys.* **87**, 247 (2015).
- [4] C. M. Surko, G. F. Gribakin, and S. J. Buckman, Low-energy positron interactions with atoms and molecules, *J. Phys. B* **38**, R57 (2005).
- [5] G. F. Gribakin, J. A. Young, and C. M. Surko, Positron-molecule interactions: Resonant attachment, annihilation, and bound states, *Rev. Mod. Phys.* **82**, 2557 (2010).
- [6] S. J. Brawley, S. Armitage, J. Beale, D. E. Leslie, A. I. Williams, and G. Laricchia, Electron-like scattering of positronium, *Science* **330**, 789 (2010).
- [7] D. B. Cassidy, Experimental progress in positronium laser physics, *Eur. Phys. J. D* **72**, 53 (2018).
- [8] The ALPHA collaboration, Confinement of antihydrogen for 1,000 seconds, *Nat. Phys.* **7**, 558 (2011).
- [9] N_2 is chosen as the buffer gas because it is the only known molecule for which the threshold for electronic excitation (≈ 8.5 eV) is sufficiently below the threshold for positronium formation (≈ 8.8 eV) [10].
- [10] S. Marjanović, A. Banković, D. Cassidy, B. Cooper, A. Deller, S. Dujko, and Z. Lj. Petrović, A CF_4 based positron trap, *J. Phys. B* **49**, 215001 (2016).
- [11] M. R. Natisin, J. R. Danielson, and C. M. Surko, A cryogenically cooled, ultra-high-energy-resolution, trap-based positron beam, *Appl. Phys. Lett.* **108**, 024102 (2016).
- [12] T. C. Griffith and G. R. Heyland, Experimental aspects of the study of the interaction of low-energy positrons with gases, *Phys. Rep.* **39**, 169 (1978).
- [13] M. Charlton, Experimental studies of positrons scattering in gases, *Rep. Prog. Phys.* **48**, 737 (1985).
- [14] P. H. R. Orth and G. Jones, Annihilation of positrons in argon II. Theoretical, *Phys. Rev.* **183**, 16 (1969).
- [15] R. I. Campeanu and J. W. Humberston, Diffusion of positrons in helium gas, *J. Phys. B* **10**, 239 (1977).
- [16] R. I. Campeanu, On the theoretical and experimental cross sections for low-energy positron-rare-gas scattering, *J. Phys. B* **14**, L157 (1981).
- [17] R. I. Campeanu, Positron diffusion in krypton and xenon, *Can. J. Phys.* **60**, 615 (1982).
- [18] B. Shizgal and K. Ness, Thermalisation and annihilation of positrons in helium and neon, *J. Phys. B* **20**, 847 (1987).
- [19] G. J. Boyle, M. J. E. Casey, R. D. White, and J. Mitroy, Transport theory for low-energy positron thermalization and annihilation in helium, *Phys. Rev. A* **89**, 022712 (2014).
- [20] D. G. Green, Positron Cooling and Annihilation in Noble Gases, *Phys. Rev. Lett.* **119**, 203403 (2017).
- [21] D. G. Green, Probing positron cooling in noble gases via annihilation γ spectra, *Phys. Rev. Lett.* **119**, 203404 (2017).
- [22] M. Girardi-Schappo, W. Tenfen, and F. Arretche, A random walk approach to the diffusion of positrons in gaseous media, *Eur. Phys. J. D* **67**, 123 (2013).
- [23] A. Banković, S. Dujko, S. Marjanović, R. D. White, and Z. Lj. Petrović, Positron transport in CF_4 and N_2/CF_4 mixtures, *Eur. Phys. J. D* **68**, 127 (2014).
- [24] As far as we are aware, the only existing calculations of positron-impact vibrational excitation of CF_4 are the Born-dipole calculation [34] and a semiempirical coupled-channel calculation [35]. for positron-impact rotational excitation of N_2 , apart from the Born-quadrupole calculation [40], other calculations present only cross sections for excitations $0 \rightarrow J$ for a few values of the angular momentum J or summed cross sections [46, 47].
- [25] M. R. Natisin, J. R. Danielson, and C. M. Surko, Positron cooling by vibrational and rotational excitation of molecular gases, *J. Phys. B* **47**, 225209 (2014).
- [26] ν_3 dominates due to its significantly larger cross section.
- [27] D. Trunec, P. Španěl, and D. Smith, The influence of electron-electron collisions on electron thermalization in He and Ar afterglow plasmas, *Chem. Phys. Lett.* **372**, 728 (2003).
- [28] J. R. Danielson, M. R. Natisin, and C. M. Surko, (2021), private communication.
- [29] D. G. Green, ANTICOOL: Simulating positron cooling and annihilation in atomic gases, *Comput. Phys. Comm.* **224**, 362 (2018).
- [30] In practice, we choose the time-density step $\Delta\tau$ small enough that $W\Delta\tau < 0.1$ is always satisfied.
- [31] Y. Weng and M. J. Kushner, Method for including electron-electron collisions in Monte Carlo simulations of electron swarms in partially ionized gases, *Phys. Rev. A* **42**, 6192 (1990).
- [32] See also `supp_info.pdf` in the Supplementary Material.
- [33] D. R. Lide, ed., *CRC Handbook of Chemistry and Physics*, 89th ed. (CRC Press, Boca Raton, FL, 2008–2009).
- [34] Y. Itikawa, The Born cross section for vibrational excitation of a polyatomic molecule by electron collisions, *J. Phys. Soc. Japan* **36**, 1121 (1974).
- [35] J. Franz, I. Baccarelli, S. Caprasecca, and F. A. Gianturco, Computed vibrational excitation of CF_4 by low-energy electrons and positrons: Comparing calculations and experiments, *Phys. Rev. A* **80**, 012709 (2009).
- [36] M. Kurihara, Z. L. Petrovic, and T. Makabe, Transport coefficients and scattering cross-sections for plasma modelling in CF_4 -Ar mixtures: a swarm analysis, *J. Phys. D* **33**, 2146 (2000).
- [37] The experiment for CF_4 used a gas pressure and temperature of 0.51 μ Torr and 300 K, respectively [25].
- [38] See also `CF4_video.mov` (https://youtu.be/BHJ5ezj1_

- 1E) in the Supplementary Material for a video showing the time evolution of $f(k, \tau)$ for cooling in CF_4 . ().
- [39] K. P. Huber and G. Herzberg, eds., *Molecular Spectra and Molecular Structure IV. Constants of Diatomic Molecules* (Van Nostrand Reinhold, New York, 1979).
 - [40] E. Gerjuoy and S. Stein, Rotational excitation by slow electrons, *Phys. Rev.* **97**, 1671 (1955).
 - [41] The experiment for N_2 used a gas pressure and temperature of $15 \mu\text{Torr}$ and 300 K , respectively [25].
 - [42] T. Mukherjee, A. S. Ghosh, and A. Jain, Low-energy positron collisions with H_2 and N_2 molecules by using a parameter-free positron-correlation-polarization potential, *Phys. Rev. A* **43**, 2538 (1991).
 - [43] I. Al-Qaradawi, M. Charlton, I. Borozan, R. Whitehead, and I. Borozan, Thermalization times of positrons in molecular gases, *J. Phys. B* **33**, 2725 (2000).
 - [44] See also N2_video.mov (https://youtu.be/wR1zdg_9gtc) in the Supplementary Material for a video showing the time evolution of $f(k, \tau)$ for cooling in N_2 .
 - [45] The annihilation cross section is $\sigma_{\text{ann}} = \pi r_0^2 c Z_{\text{eff}} / v$, where r_0 is the classical electron radius, c is the speed of light, v is the positron velocity, and Z_{eff} is the effective number of electrons contributing to annihilation. Measurements and calculations of Z_{eff} for CF_4 and N_2 indicate $Z_{\text{eff}} \sim 10^1$ for both species [13, 48, 49], which makes σ_{ann} negligible in comparison to the total vibrational (for CF_4) or rotational (for N_2) cross section [32].
 - [46] T. Mukherjee and M. Mukherjee, Low-energy positron–nitrogen-molecule scattering: A rovibrational close-coupling study, *Phys. Rev. A* **91**, 062706 (2015).
 - [47] M. V. Barp, E. P. Seidel, F. Arretche, and W. Tenfen, Rotational excitation of N_2 by positron impact in the adiabatic rotational approximation, *J. Phys. B* **51**, 205201 (2018).
 - [48] J. Marler, L. Barnes, S. Gilbert, J. Sullivan, J. Young, and C. Surko, Experimental studies of the interaction of low energy positrons with atoms and molecules, *Nucl. Instrum. Methods Phys. Res. B* **221**, 84 (2004).
 - [49] A. R. Swann and G. F. Gribakin, Model-potential calculations of positron binding, scattering, and annihilation for atoms and small molecules using a gaussian basis, *Phys. Rev. A* **101**, 022702 (2020).